Fast Metabolic Imaging of Systems with Sparse Spectra: Application for Hyperpolarized ^{13}C Imaging

D. Mayer[1], Y. S. Levin[1], G. H. Glover[1], R. E. Hurd[2], D. M. Spielman[1]

[1]Radiology, Stanford University, Stanford, CA, United States, [2]GE Healthcare, ASL-West, Menlo Park, CA, United States

Introduction

The development of hyperpolarized MRI agents presents both unprecedented opportunities as well as new technical challenges. In particular, with signal-to-noise ratio (SNR) enhancements on the order of the 100,000-fold, dynamic nuclear polarization of metabolically active substrates (e.g., ^{13}C-labeled pyruvate or acetate) (1,2) theoretically permits in vivo imaging of not only the injected agent, but also downstream metabolic products. This feature of hyperpolarized MR spectroscopy provides a unique chance to noninvasively monitor critical dynamic metabolic processes in vivo under both normal and pathologic conditions. As the hyperpolarized magnetization decays towards its thermal equilibrium value and is not recoverable, fast acquisition schemes are important. The need for speed in combination with the sparse spectra which can occur in the application of hyperpolarized ^{13}C metabolic imaging makes spiral chemical shift imaging (spCSI) (3) an ideal candidate for this application. The aim of this work was to implement a ^{13}C spCSI sequence that speeds up the acquisition by undersampling the data in the spectral domain. Prior knowledge of resonance frequencies can be exploited to minimize signal overlap.

Methods

All measurements were performed on a GE 3 T MR scanner equipped with self-shielded gradients (40 mT/m, 150 mT/m/ms). A doubly-tuned (^{1}H/^{13}C) birdcage coil (∅ = 44 mm) was used for both RF excitation and signal reception. The sequence was tested on a phantom consisting of three 2-ml vials (∅ = 10 mm) containing approximately 1.5-M ^{13}C-enriched solutions of alanine (Ala, tube 1), lactate (Lac, tube 2), and pyruvate-pyruvate hydrate C1-C2 ester (tube 3), all enriched to 99% ^{13}C in the C1 carbonyl positions. The ester has 2 resonances with frequency offsets relative to Lac of approximately -243 Hz (PPE1) and -592 Hz (PPE2), respectively.

The implemented sequence consists of a slice(z)-selective excitation (5.4 mm) and a spiral readout gradient for combined spatial(xy)-spectral(f) encoding. The spiral waveforms were designed for a FOV of 80×80 mm^2 with nominal 5×5-mm^2 in-plane resolution using an analytic algorithm (4). The spectral width (SW) was 109.7 Hz in single-interleaf mode (single-shot spCSI) and could be increased to 276.2 Hz when performing 3 spatial interleaves (3-shot spCSI). In order to increase the SNR, 60 and 30 accumulations were carried out for the two acquisition schemes, respectively. With a TR of 2 s and 8 dummy excitations, the total acquisition time (T_{acq}) was 2:16 min. The spCSI experiments were compared to conventional phase-encoded pulse-acquire CSI (FIDCSI) with the same spatial parameters (T_{acq} = 8:48 min).

Apodization of the spCSI data comprised a 5-Hz Gaussian line broadening and zero-padding up to 128 points in k_f, and multiplication with a generalized Hamming window and zero-padding up to 32×32 pixels in k_x and k_y. After FFT along k_f, a frequency-dependent linear phase-correction was applied along the readout in order to remove the chemical shift (CS) artifact. As this can not simultaneously be done for spectral components that have been aliased a different number of times, multiple data sets were reconstructed in which only components with resonance frequencies within a certain bandwidth are reconstructed "in-focus" while components outside of that band are severely blurred ("spectral tomosynthesis"). After gridding the data, a 2D-FFT was performed. Metabolic maps for Ala, Lac, PPE1, and PPE2 were calculated by integrating the signal within a 28-Hz interval around each peak in absorption mode and normalized to the maximum intensity in the PPE2 map.

Results and Discussion

Spectra acquired with single-shot spCSI from voxels located in each of the three respective tubes are shown in Fig. 1. The different line widths of the peaks are mainly due to scalar ^{13}C-^{1}H-coupling. The multiplet structure is not resolved due to the strong apodization. With the resonance frequency set to Lac, the signals from Ala and PPE1 were aliased twice and, hence, were detected at 8 Hz and -23 Hz, respectively. The PPE2 resonance was aliased five times and detected at -43 Hz. While both ester resonances are well resolved, the Ala signal severely overlaps with Lac. But since Ala is aliased twice, its PSF is blurred when the appropriate linear phase correction is applied for the reconstruction of Lac. Therefore, most of the signal in the metabolic maps of these two metabolites (Fig. 2a and 2b) falls within the respective tube, but on top of a broad, low intensity background signal. As both ester resonances are well resolved, the corresponding metabolic maps (Fig. 2c and 2d) are similar to the ones measured with FIDCSI (not shown). Due to the higher SW in the 3-shot acquisition, all 4 resonances are well resolved (Fig. 3). The resonances of Ala, PPE1, and PPE2 alias to frequencies 64 Hz, -33 Hz, and -40 Hz, respectively. The metabolic maps for all four resonances (Fig. 4) demonstrate similar resolution and localization properties as the FIDCSI images. Relative difference in amplitude ratios as measured with single-shot spCSI compared to FIDCSI are 12% for Ala/PPE2, 6% for Lac/PPE2, and 9% for PPE1/PPE2. Respective values for 3-shot spCSI are 11% for Ala/PPE2, 14% for Lac/PPE2, and 8% for PPE1/PPE2. As confirmed by simulations, the main causes of the deviations are dispersion-mode signal contributions of aliased peaks from different voxels.

Conclusion

The presented data demonstrate that spectral undersampling can be used to reduce T_{acq} of spCSI for systems with sparse spectra. When applying this technique to hyperpolarized ^{13}C metabolic imaging, no data averaging is necessary and the TR can be reduced to the minimum time necessary for excitation and data acquisition (~200-250 ms), therefore, allowing a sub-second temporal resolution. The artifacts due to the distorted PSF can potentially be reduced by using the prior knowledge of resonance frequencies, scalar coupling constants, and transverse relaxation times, and estimating the relative amplitudes with a minimum least-squares solution.

Acknowledgement

This work was supported by NIH grants RR09784, CA48269, AA12388.

References

[1] Ardenkjaer-Larsen JH et al. Proc Natl Acad Sci USA 2003;100:10158-10163. [2] in't Zandt R et al. Weekend Educational Syllabus, 13th Annual Meeting of ISMRM, Miami Beach; 2005. [3] Adalsteinsson E et al. Magn Reson Med 1998;39:889-898. [4] Glover GH. Magn Reson Med 1999;42:412-415.

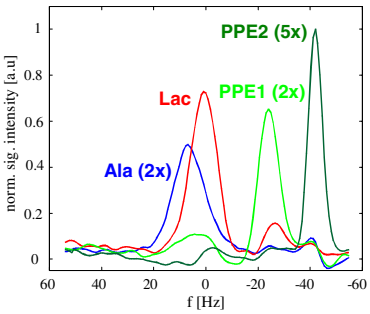

Fig. 1: Single-shot spCSI spectra from voxels in tube 1 (blue), tube 2 (red), and tube 3 (bright and dark green). The numbers indicate how often the respective component has been aliased.

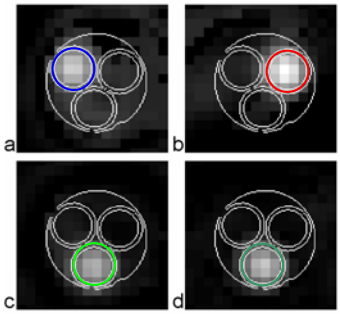

Fig. 2: Metabolic maps of Ala (a), Lac (b), PPE1 (c), and PPE2 (d) reconstructed from the single-shot spCSI data set. Contours of the phantom as derived from proton MRI are outlined.

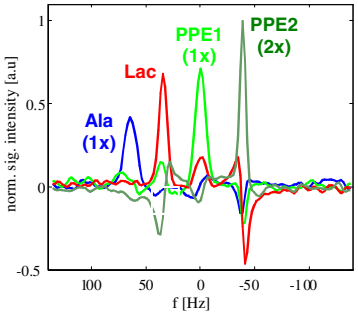

Fig. 3: 3-shot spCSI spectra from voxels in tube 1 (blue), tube 2 (red), and tube 3 (bright and dark green). The numbers indicate how often the respective component has been aliased.

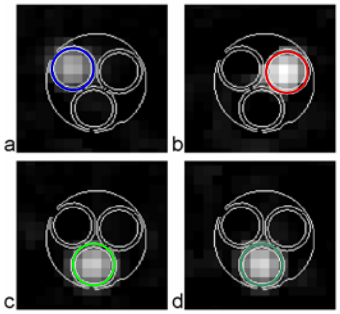

Fig. 4: Metabolic maps of Ala (a), Lac (b), PPE1 (c), and PPE2 (d) reconstructed from the 3-shot spCSI data set.